

Magnetism in the heavy-electron superconductors UPt_3 and URu_2Si_2

M. R. Norman

Materials Science Division, Argonne National Laboratory, Argonne, Illinois 60439

T. Oguchi* and A. J. Freeman

Physics and Astronomy Department, Northwestern University, Evanston, Illinois 60208

(Received 16 May 1988)

The nature of magnetism in the heavy-electron superconductors UPt_3 and URu_2Si_2 is investigated by using a spin-orbit generalized variant of local-spin-density (LSD) theory to calculate the self-consistent moment-polarized electronic structure and the dynamic (bare-band) susceptibility. It is shown that the direction of the magnetic moment is predicted correctly. The size of the moment, however, is $0.8\mu_B$ in UPt_3 and $1.2\mu_B$ in URu_2Si_2 , i.e., a factor of 40 larger than experiment. It is noted, however, that the experimental moment of $(0.65 \pm 0.1)\mu_B$ for Th- or Pd-doped UPt_3 is close to the theoretical value. The static susceptibility, $\chi(\mathbf{q})$, is predicted to be weakly dependent on \mathbf{q} except for UPt_3 , where a peak is found at $\mathbf{q}=(\pi/c)(0,0,2)$ —in general agreement with neutron-scattering data at high frequencies. The low-frequency anomalies in the neutron data which lead to magnetic ordering are not seen in the calculated dynamic susceptibility, but can be understood in terms of a moment-moment interaction. An explanation for these conflicting data is offered based on the interaction of itinerant quasiparticle and local-moment degrees of freedom at low temperatures, which leads to a renormalization of the LSD spin-spin response function.

I. INTRODUCTION

Heavy-electron metals are well known to exhibit unusual magnetic and superconducting behavior.¹ Neutron-scattering measurements have found strong antiferromagnetic correlations, even in metals which do not order magnetically.²⁻⁹ Recently, the coexistence of superconductivity and magnetism has been discovered in¹⁰ URu_2Si_2 and in³ UPt_3 . The ordered magnetic moments are very small, however, being of the order of $0.02\mu_B$ for³ UPt_3 and $0.03\mu_B$ for⁵ URu_2Si_2 . When UPt_3 is doped with¹¹ Th or with¹² Pd, the moment increases to about $0.65\mu_B$ and superconductivity disappears. The small moment, $0.02\mu_B$, in pure UPt_3 is connected with a low-frequency (0.2 meV) anomaly in the neutron-scattering data with an ordering vector of³ $(2\pi/\sqrt{3}a)(1,0,0)$. This is in contrast with the high-frequency data which reveal a peak at $(\pi/c)(0,0,2)$ with a linewidth Γ of 5 meV and a fluctuating moment of $2.1\mu_B$.² In the case of URu_2Si_2 , the magnetic transition leads to the opening of a gap over a large part of the Fermi surface, with magnon excitations propagating in the gap.^{10,4-6} In this case, the \mathbf{q} vector for ordering is $(\pi/c)(0,0,2)$.

As has been stressed by the experimentalists, the neutron-scattering data are consistent with correlated interactions of local moments.^{2,3,7,8} This is in contrast with the results of de Haas-van Alphen experiments on¹³ UPt_3 which reveal a Fermi surface consistent with that predicted by standard local-density band calculations.^{14,15} As many recent theories use the neutron-scattering susceptibility to explain the quasiparticle mass renormalizations¹⁶⁻¹⁹ and the superconducting pair instability,¹⁸⁻²¹ it is of some importance to understand the nature of the dynamic susceptibility and magnetism described above.

As a step in this direction, we have calculated the self-consistent moment-polarized electronic structure and dynamic susceptibility using a spin-orbit generalized variant of local-spin-density (LSD) theory.

In Sec. II the particular calculational procedures are outlined. In Secs. III and IV, results for UPt_3 and URu_2Si_2 , respectively, are discussed. The basic result is that although the magnetic moment directions are correctly predicted (due to simple spin-orbit effects), the calculated magnetic moments are too large by a factor of 40. A discussion of these results is given in Sec. V, where it is speculated that the calculated moments are suppressed by a correlated Kondo effect. We end in Sec. VI with some conclusions.

II. CALCULATIONAL PROCEDURE

The method used here was described in a previous paper dealing with the heavy-electron magnet UCu_5 .²² Basically, we need a formalism which can treat both spin- and orbital-moment effects. There is no exact theory for this case, but several approximate formalisms exist²³⁻²⁵ which yield good results for itinerant actinide magnets. In our case, using LSD potentials, we construct scalar relativistic (i.e., without spin-orbit) basis functions²⁶ and solve the secular matrix

$$\begin{pmatrix} H_{uu} + V_u & H_{ud} \\ H_{du} & H_{dd} + V_d \end{pmatrix}. \quad (1)$$

Here the V 's are the matrix elements involving the spin-density potentials and the H 's are the matrix elements involving the spin-orbit operator.²⁷ In the upper (lower) diagonal block, we use the V_u (V_d) potential to construct

the spin-orbit term, whereas in the off-diagonal blocks the average of the two is used. The eigenvectors of this matrix are products of scalar relativistic functions times spinors, from which new spin densities are summed and used in the next self-consistent cycle. We can also determine the orbital moment, which is $\sum_{l,m,s} mn_{l,m,s}$ where $n_{l,m,s}$ are of the lm -projected occupation numbers in each spin channel s .²³ The starting spin densities for the self-consistent calculation are obtained by taking the results of a paramagnetic calculation, and transferring a small amount of charge from one spin channel to the other.

We use the results of a fully relativistic (i.e., Dirac equation) paramagnetic calculation to construct the imaginary part of the dynamic susceptibility (without Stoner or spin-fluctuation renormalizations):

$$\begin{aligned} \text{Im}\chi(q, \omega) = & \pi \sum_{n,n'} \int d^3k f(\epsilon_{n,k}) [1 - f(\epsilon_{n',k+q})] \\ & \times \delta(\epsilon_{n',k+q} - \epsilon_{n,k} \pm \omega) \\ & \times |\langle \psi_{n,k} | \sigma e^{iq \cdot r} | \psi_{n',k+q} \rangle|^2, \end{aligned} \quad (2)$$

where n and n' are band indices, f the Fermi function, and σ the moment operator. For the real part of the susceptibility, the δ function is replaced by the inverse of its argument, and is evaluated using the tetrahedron method.²⁸ A similar method used to calculate the imaginary part involves finding the “density of states” which satisfies the δ function condition and weighting it by an average of the product of the Fermi functions. To evaluate the moment operator, we keep only the $f_{5/2}$ component of the wave functions, and treat σ as a pure j operator, replacing r in Eq. (2) by \mathbf{R} , the U-site positions. The moment operator can be expressed as a particular sum of σ_+ , σ_- , and σ_z (the coefficients depending on the direction σ are taken to point in), and the matrix elements are trivial to evaluate since the wave functions are in a pure j basis.²⁹ In practice, the matrix elements are evaluated on a regular mesh in k space which forms corners of tetrahedra, but with these tetrahedra divided into eight smaller ones when evaluating the sum in Eq. (2) (the matrix elements are linearly interpolated and the eigenvalues are evaluated from a Fourier series spline fit to the bands³⁰). Note that this restricts the q values to this mesh.

The electronic structure is calculated using the linear muffin-tin orbital (LMTO) method with combined correction terms³⁴ which correct for the nonspherical shape of the unit cell. The exchange-correlation functional used is a spin-generalized variant of the Hedin-Lundqvist form.³² For the paramagnetic calculation used as input for the dynamic susceptibility, a relativistic generalization is employed.²⁹ Basis functions up to $l=3$ were kept on the U sites, and up to $l=2$ on the other sites (for the fully relativistic UPt₃ calculation, $l=3$ basis functions were used on all sites). For the self-consistent iterations, 60 k points in the irreducible wedge were used for UPt₃, and 63 k points for URu₂Si₂. In both cases, the spline fit to the bands was generated from 120 k points, and the wavefunction mesh for the susceptibility from 75 k points (in the case of body-centered URu₂Si₂, the 75- k -point mesh

was set up in a quadruple-sized simple tetragonal irreducible wedge). For the (antiferromagnetic) moment-polarized calculations, 60 k points were used for UPt₃ in the hexagonal phase, 45 k points in the observed orthorhombic phase, and 32 k points for URu₂Si₂ in its observed tetragonal phase.

III. RESULTS FOR UPt₃

The relativistic calculation^{14,15} yields a Fermi surface in good agreement with de Haas–van Alphen (dHvA) data. As discussed in Ref. 15, combined correction terms are necessary to get the topology completely correct. Shifts of the bands of the order of 1 mRy, which are needed to get quantitative agreement with the dHvA data (these shifts are much smaller than those needed for ordinary transition metals), are incorporated when calculating the dynamic susceptibility.

The first moment-polarized calculation was done by oppositely polarizing the two U atoms in the hexagonal cell along the c axis. In all, 0.1 f electrons were transferred from the spin-up to the spin-down density when constructing the starting densities, as previous calculations indicated a sizable moment;³³ 65 iterations, however, were required to converge the moment. A total moment of $-0.27\mu_B$ per formula unit was found, with an orbital component of $-1.10\mu_B$ and a spin component of $0.83\mu_B$; virtually all the moment arises from the f electrons. Interestingly, the calculated density of states (DOS) at E_F was practically the same as in the paramagnetic case.

As a test, a new calculation was begun by transferring only 0.01 f electrons between spin channels. This time, the orbital magnetic moment was appreciably larger than an parallel to the spin moment on the first iteration. This forced the spin moment to flip direction one of the subsequent iterations. Surprisingly, the solution (after 32 iterations) converged to a different total-moment value of $0.54\mu_B$, with an orbital moment of 1.64 and a spin moment of -1.10 . Several other runs were begun using different perturbing starts, which indicated that these were the only two solutions. (It is conceivable that the previous low-moment solution is due to a poor path in configuration space, given the slow convergence of the moment in that case.) Next, the magnetic moments from the $-0.25\mu_B$ calculation were rotated along the a axis, and an additional 13 iterations were performed (the last one using 120 k points). The moment increased to $-0.71\mu_B$ (with $-1.78\mu_B$ orbital and $1.07\mu_B$ spin), suggesting (as observed experimentally) that the moments tend to lie along the a axis. (This will be verified below when the dynamic susceptibility is calculated.) Similar results were obtained when the $0.54\mu_B$ solution was used for a starting configuration.

The observed orthorhombic magnetic phase of UPt₃ corresponds to doubling the unit cell along the a axis, with the moment aligned along this axis with $\mathbf{q} = (2\pi/\sqrt{3}a)(1,0,0)$.^{3,11,12} We again took the spin densities from the $-0.25\mu_B$ calculation and rotated them along the a axis, then restarted the calculation in the or-

thorhombic phase. Eight iterations were performed, the final one using a larger 90- k -point mesh, resulting in a total moment of $-0.81\mu_B$ ($-1.98\mu_B$ orbital, $1.17\mu_B$ spin). Since the charge density still has the same (hexagonal) symmetry in both cases, the increase of the moment by $0.1\mu_B$ may suggest that the orthorhombic structure is preferred over the hexagonal one, as observed experimentally. (To verify this point would require calculating the total energy very precisely, a near impossible task for such a complex unit cell.)

Next, the dynamic susceptibility was calculated from the six $j = \frac{5}{2}$ f bands in the vicinity of E_F . Results for the static susceptibility for various \mathbf{q} vectors and moment directions are shown in Table I. One sees from the table that the susceptibility is maximal for the moment along the a axis, indicating that the a axis is the favored moment direction. One also finds a peak in $\chi(\mathbf{q})$ at $(\pi/c)(0,0,2)$, in agreement with neutron-scattering data.² Nothing special happens, however, at $\mathbf{q}=(2\pi/\sqrt{3}a,0,2\pi/c)$ (results with $q_z=0$ are very similar). To further investigate this, we calculated $\text{Im}\chi(\mathbf{q},\omega)$ for the three \mathbf{q} vectors in Table I (with the moment along a). The results are shown in Fig. 1. One sees a broad response function in all cases (when comparing to experiment, one must remember that the frequency scale in Fig. 1 will be renormalized by exchange-correlation and spin-fluctuation effects). Note that at $\mathbf{q}=\mathbf{0}$, there is interband weight at nonzero frequencies due to spin-orbit effects. In fact, the intraband contributions to $\chi(\mathbf{q})$ only amount to about 15–20% of the total.

IV. RESULTS FOR URu₂Si₂

Fully relativistic paramagnetic calculations were performed for body-centered tetragonal URu₂Si₂ with and without combined correction terms. The latter are found to be very important, as seen from the fact that the DOS at E_F doubled with their inclusion (from 8 to 17 mJ/mol K²). Four bands are found to cross E_F , with a small and large electron pocket at Γ , two hole pockets about Z , and a rather complicated piece about the $X(1,1,0)$ points. This latter piece is sensitive to the location of E_F .

The observed magnetic phase is a simple antiferromagnetic tetragonal structure with moments pointing along the c axis.⁵ The moment-polarized calculation was begun by transferring 0.01 f electrons from the up to the down

TABLE I. Calculated static susceptibility of UPt₃ for various moment directions ($\hat{\mu}$). Units are states/(Ry cell) (note, there are two U atoms per cell). The b axis is one of the hexagonal vectors in the basal plane, the a axis being orthogonal to it. The \mathbf{q} vector is in units of $2\pi\sqrt{3}a$ for q_x and π/c for q_z . Results for $\mathbf{q}=(1,0,0)$ are similar to $\mathbf{q}=(1,0,2)$.

\mathbf{q}	$\hat{\mu}\parallel c$	$\hat{\mu}\parallel a$	$\hat{\mu}\parallel b$
(0,0,0)	413	410	410
(0,0,1)		525	
(0,0,2)	530	552	552
(1,0,2)	421	520	459

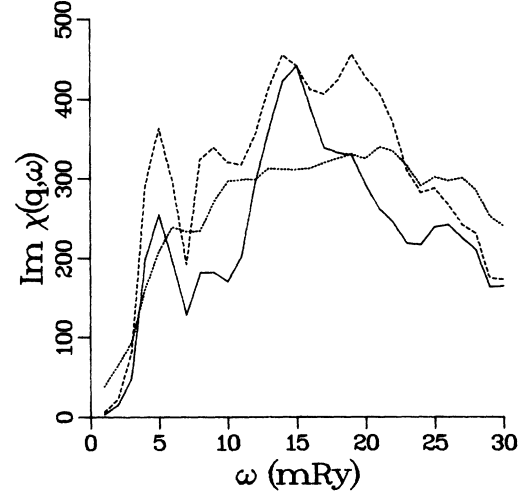


FIG. 1. Calculated imaginary susceptibility vs frequency of UPt₃. Same units as in Table I. The solid curve is for $\mathbf{q}=(0,0,0)$, the dashed curve for $\mathbf{q}=(0,0,2)$, and dotted curve for $\mathbf{q}=(1,0,2)$.

spin density. The moment converged after 40 iterations to a value of $-1.17\mu_B$ ($-2.85\mu_B$ orbital, $1.68\mu_B$ spin). The DOS at E_F was reduced by about 50% as compared to that of the paramagnetic phase. This is comparable to what is indicated by specific-heat data.¹⁰ It is interesting to note, however, that the DOS reduction only occurred once the magnetic moment began to exceed $1\mu_B$ in the self-consistent cycling.

Next, the static susceptibility was calculated from the relativistic paramagnetic calculation. The results are shown in Table II. Again, one finds that the moment direction seen experimentally (c axis) is predicted. This time, the \mathbf{q} dependence is weak (but note that there is only one U atom in the primitive cell in this case). Again, nothing special happens at either $\pi/c(0,0,2)$ or $\pi/a(2,0,0)$, which are the (equivalent) ordering vectors for URu₂Si₂. This was also found in the case of UCu₅.²²

V. DISCUSSION

We have a conflicting body of information to resolve. On the one hand, the electronic-structure calculations do well in estimating the equilibrium lattice constants for

TABLE II. Calculated static susceptibility of URu₂Si₂ for moment directions along the a and c axis. Units are states/(Ry cell). The \mathbf{q} vector units are π/a for q_x and q_y , and π/c for q_z .

\mathbf{q}	$\hat{\mu}\parallel c$	$\hat{\mu}\parallel a$
(0,0,0)	260	164
(0,0,1)	233	
(1,0,0)	266	
(2,0,0)	234	152
(1,1,0)	248	
(1,1,1)	233	

UPt₃ (Ref. 33) and UBe₁₃,³⁴ indicating that the *f* electrons participate in the bonding. In the one case where dHvA data is available, UPt₃, the correct quasiparticle Fermi surface was also found.¹³⁻¹⁵ In the case of heavy-electron magnets such as NpSn₃,²⁵ UCu₅,²² and TmSe,³⁵ moment values in good agreement with experiment are found (modulo multiplet effects in TmSe), and reasonable DOS reductions are calculated due to the lowering of symmetry in the magnetic phase. In these metals, the local-density estimate of the Stoner product, $IN(E_F)$ [where *I* is the electron-electron exchange interaction, and $N(E_F)$ the DOS at E_F], exceeds 3 [recall that $IN(E_F) > 1$ is the condition for magnetism]. We also find moment directions in agreement with experiment for UCu₅,²² UPt₃, and URu₂Si₂. Additionally, the calculated dynamic susceptibility is similar to high-frequency neutron-scattering data in that a broad frequency spectrum is predicted with a weak *q* dependence [except for UPt₃, where the two U atoms per primitive cell allow a peak at $(\pi/c)(0,0,2)$].

On the other hand, the neutron-scattering spectrum has a Lorentzian behavior with a characteristic energy (linewidth) measuring the relaxation time of the local moments; the linewidth Γ corresponds to the Curie temperature extracted from the high-temperature susceptibility.⁹ This linewidth acts as an effective Fermi temperature; for UPt₃, the ratio of the band structure E_F (~ 1000 K) to the mass renormalization factor ($=17.3$) from specific heat is 5 meV. This is Γ for UPt₃. [A proper renormalization of Fig. 1 involving the exact electron-electron exchange interaction function, $I(q, \omega, T)$, including fluctuation effects, must yield the correct behavior. We have determined that approximating $I(q, \omega)$ by $I(q)$, however, will not work for the UPt₃ case.] Moreover, low-frequency anomalies are seen in UCu₅,⁹ U₂Zn₁₇,⁹ and UPt₃ (Ref. 3) which are related to the magnetic ordering [similar low-frequency anomalies are also seen in UBe₁₃ (Ref. 36)]. These occur at *q* vectors not indicated by the calculated static susceptibility, although they are suggested by the polarized calculations (as seen above for UPt₃). Finally, moment suppression is seen in UPt₃ (Ref. 3) and URu₂Si₂ (Ref. 5), and no detectable moments have been found (yet) in UBe₁₃ and USn₃. In these four cases, the calculated Stoner products range from 1 to 2, indicating that the static magnetic correlations are weaker than in magnets such as NpSn₃ and UCu₅, where reasonable moment values were calculated.

One resolution of these problems is to speculate that the moment degrees of freedom separate from the charge degrees of freedom at high temperatures.^{18,37,38} This would explain the free-moment behavior and large entropies recovered at high temperatures, as well as the observed Schottky anomalies in the specific heat. This would also explain why one sees local-moment behavior in the measured dynamic susceptibility, yet sees a quasiparticle Fermi surface in agreement with electronic-structure calculations. As the temperature is lowered, these local moments begin to interact with each other and with the charge degrees of freedom in a coherent fashion, leading to large mass renormalizations of the

quasiparticles,¹⁶⁻¹⁹ and in most cases to a superconducting pairing instability¹⁸⁻²¹ and/or magnetic ordering.

A proposed theory for describing these dynamic interactions is the correlated Kondo approach.^{37,38,18} This would explain the suppressed (ordered) moments seen in UPt₃ and URu₂Si₂. If the static magnetic correlations are too large (or the correlated Kondo effect is destroyed by impurities), then the full band-structure moment develops, as seen in magnets such as UCu₅, and in doped UPt₃. This moment suppression can also be turned off by a field, as seen in URu₂Si₂,³⁹ where the moment jumps by about $1\mu_B$ between 35 and 40 T (the electronic structure moment being $1.2\mu_B$), and in UPt₃, where the moment jumps by $0.6\mu_B$ at ~ 20 T. There is also a simple way to determine the ordering vector. Take the *q* vector to be along the moment direction, with the magnitude arranged to give the simplest antiferromagnetic ordering along that direction. This works for UCu₅,⁴¹ U₂Zn₁₇,⁴² NpSn₃,²⁵ UPt₃,^{11,12} and URu₂Si₂.⁵ Thus the ordering is due to a moment-moment interaction (note that spin-orbit effects, which determine the direction of the moment, are crucial). This effect is not present in Eq. (2). As noted in Sec. III, however, self-consistent polarized calculations did suggest the proper *q* vector for UPt₃. This implies: (1) the *q* vector is indeed determined by $I(\mathbf{q})$ as opposed to $\chi_0(\mathbf{q})$, and (2) this effect is being reproduced by the polarized calculations (modulo *a* moment renormalization). Taken together, this indicates the possibility that $I(\mathbf{q})$ could be calculated by appropriately (Kondo) renormalizing a spin-orbit generalized variant of the LSD derived $I(\mathbf{q})$.

Finally, we note that the Néel temperature has been estimated successfully for UCu₅ using the Moriya spin-fluctuation theory.²² Until this theory is generalized to noncubic cases (where the susceptibility is directionally dependent above T_N), we cannot make an accurate estimate of T_N for UPt₃. Since T_N is proportional to $\Gamma^{1/3}$ and $M^{4/3}$ (where *M* is the magnetic moment), reasonable T_N values for UPt₃ can only be obtained if the high-frequency Γ and the nonsuppressed moment are used. To understand this, we note that there are three contributions to the spin-spin response function: I_{XC} , I_{SF} , and I_{CK} , with I_{XC} being the LSD part, I_{SF} the spin fluctuation part, and I_{CK} the correlated Kondo part. Now, I_{CK} acts to renormalize I_{XC} downwards, and thus reduces the ordered moment. I_{SF} , on the other hand, acts to renormalize the Stoner temperature down to the actual Néel temperature.³¹ This could explain why T_N is only weakly affected by doping, whereas the magnetic moment is strongly affected.

There are still some loose ends concerning URu₂Si₂. In this case, magnetic ordering is speculated to cause a gap over most of the Fermi surface, which is reflected by a gap in the magnetic excitation spectrum (in which magnons propagate).^{10,4,5} This view is difficult to resolve with the results of the moment-polarized calculation which indicates gapping only when the moment exceeds $1\mu_B$, and the calculated static susceptibility which indicates no Fermi-surface nesting. A possible resolution of this problem is to speculate that the gap is only in the

moment degrees of freedom. The differences observed in the magnetic properties of URu_2Si_2 as compared to the rest of the heavy-electron magnets indicate that the correlated interactions of the moments can lead to quite complex behavior.

VI. CONCLUSIONS

Results of moment-polarized local-density calculations on UPt_3 and URu_2Si_2 have been discussed in light of experimental data. Although the directions of the magnetic moments are correctly predicted, the calculated moments are a factor of 40 larger than experiment. Moreover, although the calculated q dependence of the susceptibility is consistent with high-frequency neutron-scattering data, it is not consistent with the observed ordering vector. The observed ordering vectors, however, appear to be consistent with the polarized calculations, where the suppressed magnetic moments are consistent with a correlated Kondo interaction among the moments. The moment suppression can be destroyed by doping or by a field, which leads to a recovery of the full electronic-

structure moment. This moment reduction is necessary so as to suppress the static magnetic correlations indicated by the electronic-structure calculations, which in turn allows a superconducting state to develop from the dynamic magnetic correlations at low temperatures.

ACKNOWLEDGMENTS

We gratefully acknowledge an extended discussion with Professor D. Pines and Professor C. Pethick, which helped greatly in writing the discussion section. The authors also acknowledge helpful correspondence with Dr. C. Broholm and Dr. A. deVisser. Work at Argonne National Laboratory was supported by the U.S. Department of Energy, Office of Basic Energy Sciences, under Contract No. W-31-109-ENG-38, and a grant of computer time at the Energy Research Cray-XMp and Cray-2 at the Magnetic Fusion Energy Computing Center, the Air Force Weapons Laboratory Cray 2, and at Northwestern University by the National Science Foundation (DMR Grant No. 85-18607).

*Present address: National Research Institute for Metals, Tokyo, Japan.

- ¹G. R. Stewart, *Rev. Mod. Phys.* **56**, 755 (1984); H. R. Ott, in *Progress in Low Temperature Physics*, edited by D. F. Brewer (North-Holland, New York, 1987), Vol. 11, p. 215; Z. Fisk, D. W. Hess, C. J. Pethick, D. Pines, J. L. Smith, J. D. Thompson, and J. O. Willis, *Science* **239**, 33 (1988).
- ²G. Aeppli, A. Goldman, G. Shirane, E. Bucher, and M.-Ch. Lux-Steiner, *Phys. Rev. Lett.* **58**, 808 (1987); A. I. Goldman, G. Shirane, G. Aeppli, E. Bucher, and J. Hüfnagl, *Phys. Rev. B* **36**, 8523 (1987).
- ³G. Aeppli, E. Bucher, C. Broholm, J. K. Kjems, J. Baumann, and J. Hüfnagl, *Phys. Rev. Lett.* **60**, 615 (1988); P. Frings, B. Renker, and C. Vettier, *Physica B* **151**, 499 (1988).
- ⁴U. Walter, C.-K. Loong, M. Loewenhaupt, and W. Schlabitz, *Phys. Rev. B* **33**, 7875 (1986).
- ⁵C. Broholm, J. K. Kjems, W. J. L. Buyers, P. Matthews, T. T. M. Palstra, A. A. Menovsky, and J. A. Mydosh, *Phys. Rev. Lett.* **58**, 1467 (1987).
- ⁶E. Holland-Moritz, W. Schlabitz, M. Loewenhaupt, U. Walter, and C.-K. Loong, *J. Magn. Magn. Mater.* **63-64**, 187 (1987).
- ⁷G. Aeppli, H. Yoshizawa, Y. Endoh, E. Bucher, J. Hüfnagl, Y. Onuki, and T. Komatsubara, *Phys. Rev. Lett.* **57**, 122 (1986).
- ⁸C. Broholm, J. K. Kjems, G. Aeppli, Z. Fisk, J. L. Smith, S. M. Shapiro, G. Shirane, and H. R. Ott, *Phys. Rev. Lett.* **58**, 917 (1987).
- ⁹U. Walter, M. Loewenhaupt, E. Holland-Moritz, and W. Schlabitz, *Phys. Rev. B* **36**, 1981 (1987).
- ¹⁰T. T. M. Palstra, A. A. Menovsky, J. van den Berg, A. J. Dirkmaat, P. H. Kes, G. J. Nieuwenhuys, and J. A. Mydosh, *Phys. Rev. Lett.* **55**, 2727 (1985); M. B. Maple, J. W. Chen, Y. Dalichaouch, T. Kohara, C. Rossel, M. S. Torikachvili, M. W. McElfresh, and J. D. Thompson, *ibid.* **56**, 185 (1986); W. Schlabitz, J. Baumann, B. Pollit, U. Rauchschwalbe, H. M. Mayer, U. Ahlheim, and C. D. Bredl, *Z. Phys. B* **62**, 171 (1986).
- ¹¹A. I. Goldman, G. Shirane, G. Aeppli, B. Batlogg, and E.

Bucher, *Phys. Rev. B* **34**, 6564 (1986).

- ¹²P. H. Frings, B. Renker, and C. Vettier, *J. Magn. Magn. Mater.* **63-64**, 202 (1987).
- ¹³L. Taillefer, R. Newbury, G. G. Lonzarich, Z. Fisk, and J. L. Smith, *J. Magn. Magn. Mater.* **63-64**, 372 (1987); L. Taillefer and G. G. Lonzarich, *Phys. Rev. Lett.* **60**, 1570 (1988).
- ¹⁴T. Oguchi, A. J. Freeman, and G. W. Crabtree, *J. Magn. Magn. Mater.* **63-64**, 645 (1987).
- ¹⁵C. S. Wang, M. R. Norman, R. C. Albers, A. M. Boring, W. E. Pickett, H. Krakauer, and N.E. Christensen, *Phys. Rev. B* **35**, 7260 (1987); M. R. Norman, R. C. Albers, A. M. Boring, and N. E. Christensen, *Solid State Commun.* **68**, 245 (1988).
- ¹⁶G. G. Lonzarich, *J. Magn. Magn. Mater.* **54-57**, 612 (1986).
- ¹⁷R. Konno and T. Moriya, *J. Phys. Soc. Jpn.* **56**, 3270 (1987).
- ¹⁸C. J. Pethick and D. Pines, in *Novel Superconductivity*, edited by S. A. Wolf and V. Z. Kresin (Plenum, New York, 1987), p. 201.
- ¹⁹M. R. Norman, *Phys. Rev. Lett.* **59**, 232 (1987); M. R. Norman, *Phys. Rev. B* **37**, 4987 (1988).
- ²⁰K. Miyake, S. Schmitt-Rink, and C. M. Varma, *Phys. Rev. B* **34**, 6554 (1986).
- ²¹W. Putikka and R. Joynt, *Phys. Rev. B* **37**, 2372 (1988).
- ²²M. R. Norman, B. I. Min, T. Oguchi, and A. J. Freeman *Phys. Rev. B* **38**, 6818 (1988).
- ²³M. S. S. Brooks and P. S. Kelly, *Phys. Rev. Lett.* **51**, 1708 (1983); M. S. S. Brooks, *Physica B+C* **130B**, 6 (1985).
- ²⁴G. Schadler, P. Weinberger, A. M. Boring, and R. C. Albers, *Phys. Rev. B* **34**, 2 (1986).
- ²⁵M. R. Norman and D. D. Koelling, *Phys. Rev. B* **33**, 3803 (1986).
- ²⁶B. N. Harmon and D. D. Koelling, *J. Phys. C* **7**, L210 (1974).
- ²⁷A. H. MacDonald, W. E. Pickett, and D. D. Koelling, *J. Phys. C* **13**, 2675 (1980).
- ²⁸J. Rath and A. J. Freeman, *Phys. Rev. B* **11**, 2109 (1975).
- ²⁹C. Godreche, *J. Magn. Magn. Mater.* **29**, 262 (1982).
- ³⁰D. D. Koelling and J. H. Wood, *J. Comput. Phys.* **67**, 253 (1986).

- ³¹O. K. Andersen, *Phys. Rev. B* **12**, 3060 (1975).
- ³²L. Hedin and B. I. Lundqvist, *J. Phys. C* **4**, 2064 (1971).
- ³³J. Sticht and J. Kubler, *Solid State Commun.* **54**, 389 (1985).
- ³⁴W. E. Pickett, H. Krakauer, and C. S. Wang, *Physica B+C* **135B**, 31 (1985).
- ³⁵M. R. Norman and H. J. F. Jansen, *Phys. Rev. B* **37**, 10050 (1988).
- ³⁶A. I. Goldman, *Suppl. Jpn. J. Appl. Phys.* **26-3**, 1887 (1987).
- ³⁷B. A. Jones and C.M. Varma, *Suppl. Jpn. J. Appl. Phys.* **26-3**, 1875 (1987); R. M. Fye, J. E. Hirsch, and D. J. Scalapino, *Phys. Rev. B* **35**, 4901 (1987); C. Jayaprakash, H. R. Krishna-murthy, and J. W. Wilkins, *Phys. Rev. Lett.* **47**, 737 (1981).
- ³⁸C. M. Varma, *Comments Solid State Phys.* **11**, 5 (1985); P. W. Anderson, in *Theoretical and Experimental Aspects of Valence Fluctuations and Heavy Fermions*, edited by L. C. Gupta and S. K. Malik (Plenum, New York, 1987), p. 1.
- ³⁹A. deVisser, F. R. de Boer, A. A. Menovsky, and J. J. M. Franse, *Solid State Commun.* **64**, 527 (1987).
- ⁴⁰P. H. Frings and J. J. M. Franse, *Phys. Rev. B* **31**, 4355 (1985).
- ⁴¹A. Murasik, S. Ligenza, and A. Zygmunt, *Phys. Status Solidi A* **23**, K163 (1974).
- ⁴²D. E. Cox, G. Shirane, S. M. Shapiro, G. Aeppli, Z. Fisk, J. L. Smith, J. Kjems, and H. R. Ott, *Phys. Rev. B* **33**, 3614 (1986).